IOP Conf. Series: Materials Science and Engineering **168** (2017) 012044 doi:10.1088/1757-899X/168/1/012044

Numerical simulation of discharge plasma generation and nitriding the metals and alloys

T V Koval[1], R A Manakov[2], Nguyen Bao Hung[3] and Tran My Kim An[4]

[1] Professor, National Research Tomsk Polytechnic University, 30, Lenin Ave., Tomsk, 634050, Russia.
[2] Student, National Research Tomsk Polytechnic University, 30, Lenin Ave., Tomsk, 634050, Russia.
[3,4] Post-graduate students, National Research Tomsk Polytechnic University, 30, Lenin Ave., Tomsk, 634050, Russia.

Email: tvkoval@mail.ru

Abstract. This research provides the numerical simulation of the plasma generation in a hollow cathode as well as the diffusion of nitrogen atoms into the metal in the low-pressure glow discharge plasma. The characteristics of the gas discharge were obtained and the relation of the basic technological parameters and the structural and phase state of the nitrided material were defined. Authors provided the comparison of calculations with the experimental results of titanium nitriding by low-pressure glow discharge plasma in a hollow cathode.

1. Introduction

The ion-plasma surface treatment in plasma gas discharge, particularly the nitriding treatment have been increasingly developed [1-9] in recent years. The vacuum plasma technology on the ground of low temperature glow discharge plasma is used for the surface modification of materials and bulk items [4-9], when the ion current density of ~ 1 mA/cm^2 over the treated surface as well as the discharge voltage of hundreds volt to be provided [8-11].

The target material for plasma treatment is immersed into the gas plasma where ions accelerated towards the target in the double electric layer between the target and the discharge column. A treating agent (gas atoms) is propagated in the target material due to the activated thermal diffusion which rate is dependent on the temperature of the treatment and the agent density distribution profile. The main parameters for the plasma treatment are gas mixture, temperature and time of the process, operating pressure, ion current density to the target surface and the ion energy. Most of the parameters are interdependent. Therefore, the proportion of components in gas mixture impacts the voltage, which triggers the discharge, and the ion energy as well. The voltage and the current density are bounded with the value of the allowed treatment temperature and the gas pressure. The nitriding in the range of 200-300 °C provides the solid nitride layers up to 500 μm thick [4, 5].

The multiple complex processes, which take place during the nitriding, make it difficult to reveal the common trends in structuring the modified layers and their characteristics [11-14]. Simulating the processes, which occur during the plasma generation and nitriding of materials, provides the efficient opportunity to identify the mechanism of the modified layer formation with predefined characteristics and their relation to the technological parameters such as gas type and pressure, discharge current and

voltage, ion current density. It is fair to assume that the precise quantitative ratio of process parameters and the phase-structural condition of the material surface will help to improve the established nitriding techniques and develop new ways of modification based on the data available.

The current research provides the simulation of plasma generation with the non-self-sustained glow discharge in a hollow cathode at the low gas pressure as well as the diffusion penetration of the nitrogen atoms into the metal. The authors also made a comparison of the numerical simulation with the nitriding of titanium in the real experiment.

2. Simulation of gas discharge in a hollow cathode

As the experiments [8, 9] demonstrated, plasma was generated in a hollow cylindrical cathode (figure 1). The anode *1*, a set of two tubes with a total area of S_a, is located at the side face of the cathode, which hollow volume is $V_c = 2\times10^5$ cm^3, S_a = 125-500 cm^2. Plasma might be generated in the main self-sustained discharge mode and in the electron beam assisted discharge mode. In latter case, the electron beam is extracted from plasma of the auxiliary arc discharge *3*. Plasma is generated inside the hollow cathode, the cathode voltage drop U_c is about the discharge voltage U. The plasma ions accelerated in the cathode layer provide the ion-electron emission from the cathode surface. The electrons, oscillating in the hollow cathode, ionize the gas and provide the discharge self-sustainability.

The equation for the main discharge in non-self-sustained mode can be obtained from the equation of the high-energy electron balance

$$u = \frac{P}{P(\gamma+\delta)-1}, \tag{1}$$

which combines the dimensionless discharge voltage $u = e\,U_c/W$, gas pressure $P = (p/kT_e)\sigma_i L$ and the effective length of the hollow cathode $L = 4V/S_a$, where W – total energy loss of an electron during the gas ionizing; γ – the coefficient of the ion-electron emission; δ – the ratio of the external electron current involved in ionization to the discharge current; V – the cathode effective volume with targets; σ_i – the cross-section of the gas ionization with electrons.

To define the spatial distribution of the electron temperature and plasma concentration as well as the impact of geometry, the size and material of the parts immersed into the hollow cathode the numerical model was used that described the density of electrons (n_e) and their average energy (n_ε) as the temporal and spatial functions [9].

$$\frac{\partial n_{e,\varepsilon}}{\partial t} + \nabla\vec{\Gamma}_{e,\varepsilon} + \vec{E}\cdot\vec{\Gamma}_{e,\varepsilon} = R_{e,\varepsilon}, \quad \vec{\Gamma}_{e,\varepsilon} = -\left(\mu_{e,\varepsilon}\cdot\vec{E}\right)n_{e,\varepsilon} - D_{e,\varepsilon}\cdot\nabla n_{e,\varepsilon} \tag{2}$$

where $\vec{\Gamma}_{e,\varepsilon}$ – flows of electrons and energy, $\mu_{e,\varepsilon}$ – mobility, $\vec{E}$ – electrical field, $D_{e,\varepsilon}$ – diffusion coefficients, $R_{e,\varepsilon}$ – the ionization rate and energy loss/gain of electrons due to the non-elastic collisions. The plasma generation in the hollow cathode was simulated regardless of the collisionless layer of the positive charge, which separates the cathode sides and targets from the plasma column. On condition of the current continuity at the computational domain boundaries, the input parameters for the numerical model are the discharge characteristics obtained from the model (1).

The high voltage of the main discharge in the self-sustained mode is the disadvantage of the hollow cathode technique since it results in the intensive ion-beam etching of the treated surface. As is shown in the equation (1) and figure 2, the characteristic of the main discharge tends to the lower voltage and gas pressure, when the auxiliary discharge is present. Figure 2 presents the calculated (by 1) and the experimental [8, 9] relations between the discharge voltage and the gas (nitrogen) pressure at different effective lengths of the hollow cathode $L = 4V/S_a$ and a discharge current of 30 A. Reducing the effective length of the hollow cathode $L = 4V/S_a$ (by extending anode area S_a or reducing the cathode volume due to targets $V_c - V_d$) as well as the decline of the operation pressure of the main discharge

results in the increase of discharge voltage. It occurs due to the deposition of the high-energy electrons to the anode. The predefined current of the self-sustained discharge is provided by the emission current (due to the coefficient γ_{N_2} = 0.04-0.2).

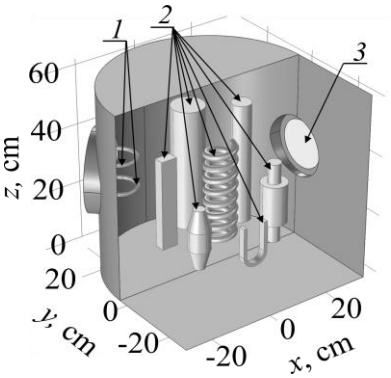

Figure 1. Hollow cathode model: *1* – anode; *2* – targets; *3* – auxiliary discharge window.

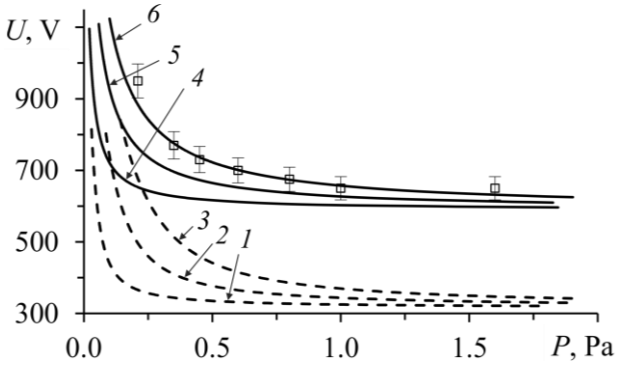

Figure 2. Dependence of discharge voltage on gas (nitrogen) pressure in non-self-sustained (*1,2,3*) (δ = 0.11) and self-sustained discharge (*4,5,6*) modes; *1,4* – $L = 6.4\times10^3$cm; *2,5* – 4.0×10^3cm; *3,6* – 1.6×10^3cm; ⫲ – experiment; I = 30 A.

The numerical simulation revealed that the plasma concentration was about 10^{11} cm^{-3} (nitrogen) under the discharge voltage of 300-400 V and the gas pressure of 0.65 Pa. The plasma temperature was within the order of 1 eV.

The control of the ion current density and the main discharge voltage could be provided by the external injection current without regard to the surface area and target material. The dependence of the discharge voltage U on the volume of target specimen (figure 3) was altered inessentially in the self-sustained as well as in the non-self-sustained discharge under the nitrogen pressure of p_{N2}>0.65 Pa.

The dependence of the external injection current and the plasma potential on the number of treated targets N for p_{N_2} = 0.65 Pa is shown in figure 4. The discharge voltage of 370 V and the ion current density was stabilized when increasing the number of targets (N = 1-8) by changing the external emission current from 9 to 14 A. The plasma potential slightly increased since $(V_c - V_d) << V_c$ (figure 4), the total target volume was $(0.25\text{-}2)\times10^4$ cm^3, the relative surface area of the target parts was S_d/S_c = 0.071-0.57.

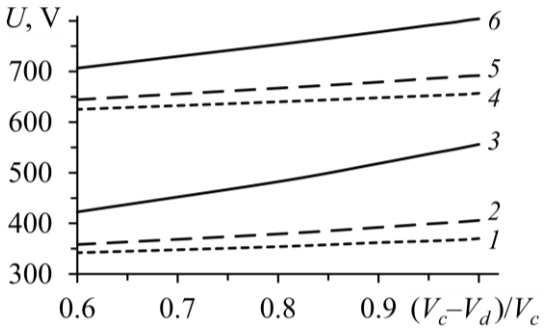

Figure 3. Discharge voltage in nitrogen vs. the relative volume in the non-self-sustained (*1,2,3*) and self-sustained (*4,5,6*) modes; *1,4* – p = 1; *2,5* – 0.65; *3,6* – 0.35 Pa; δ = 0.11.

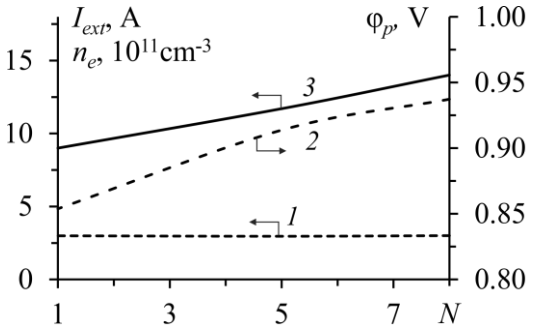

Figure 4. Plasma density (*1*), plasma potential (*2*) and external injection current (*3*), vs. the number of targets; working gas – nitrogen.

The shape of the targets and their positioning relatively to the cathode surface impact the flow density of the accelerated ions to the surface of the treated targets and the nitriding uniformity, respectively. The calculated lines of the plasma concentration level when I_{ext} = 14 A and U = 370 V in two cross sections of the hollow cathode are presented in figure 5. The small gradient in plasma concentration occurred around the emission window due to the external injection electrons. The calculations suggested that the change in the distance between the target frame and the cathode side from 5 mm to 2 mm resulted in the halving of the plasma concentration near the target's end face with respect to the face side.

During the treatment, the target was used as a cathode. A space charge layer formed between the plasma and the target, and the plasma ions accelerated in the electric field of the charge. The targets were heated due to the ion impact. The numerical solution of the heat conduction problem with regard to the water cooling of the cathode walls (figure 1) was performed for the Ti and Fe targets of ∅ = 5-13 cm and l = 20-40 cm in size.

The calculations demonstrated that using the active screen placed 2 cm apart from the cathode and around all targets led to the time reduction of the target heating up to 400 °C for 1 hour (figure 6). That provided the time difference in the nitriding as well as in the nitrogen penetration depth. The control of the target heating was performed by the external injection current and by auxiliary screens as well.

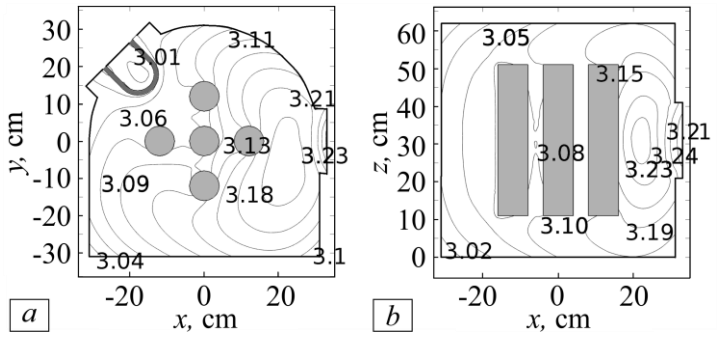

Figure 5. Plasma density distribution for nitrogen ($cm^{-3}\times10^{11}$) in the lateral (*a*) and longitudinal (*b*) sections of the hollow cathode with targets; non-self-sustained mode.

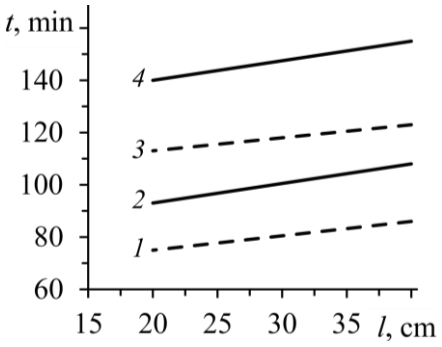

Figure 6. Heating time vs. detail length; *1,3* – ∅ = 10 cm; *2,4* – 13 cm; *1,2* – Ti; *3,4* – Fe.

The discharge condition (1) and the numerical simulation of plasma generation (2) make it possible to determine the technological parameters such as gas pressure, ion current density and discharge voltage required for the plasma treatment of the target parts.

3. Simulation of diffusion and kinetic processes

The experiment demonstrated that the increase of the nitrogen concentration correlates to the increase of the surface microhardness, and the thickening the nitrated layer provides the increase of durability [6, 7]. Currently, there is no universal model, which explains the process of the material nitriding by the discharge plasma treatment. One of the perspective approaches to clarify the nitriding process is as follows: the main part in the process belongs to atomic nitrogen, and the nitriding intensity in a glow discharge is defined by the amount of atomic nitrogen [11]. Considering that the increase of nitride layers is controlled by the diffusion of the nitrogen atoms, let us take a look at the following diffusion model:

$$\frac{\partial C}{\partial t} = \frac{\partial}{\partial x} D \frac{\partial C}{\partial x}. \qquad (3)$$

where $C = C(x, t)$ is the nitrogen concentration when the ion nitriding of the metal, $D = D_0\exp(-E_a/RT)$ is the nitrogen diffusion coefficient dependent on the temperature T and concentration C, R is the gas

constant, E_a is the energy of the diffusion activation. When simulating the diffusion of nitrogen to titanium, the initial condition $C(0, t) = 0$ and the third boundary condition were used:

$$-D\frac{\partial C(x=0,t)}{\partial x} = \alpha(C_S - C), \qquad -D\frac{\partial C(x=l,t)}{\partial x} = 0, \tag{4}$$

where α is the effective mass transfer coefficient; C_S is the nitrogen concentration at the target surface.

Experimentally [6], the microhardness profiles for the near-surface layers of titanium BT1-0 were obtained. The titanium BT1-0 was nitrided in the non-self-sustained glow discharge plasma with a hollow cathode under a low pressure and different temperatures T = 550, 650, 850 °C during five hours (figure 7). The backside of the specimen was positioned at the distance of 0.5 mm from the hollow cathode surface. The microhardness was tested from both sides of the specimen. The experimental results on the surface microhardness of the titanium test objects treated under different parameters of the glow discharge and the nitriding temperature demonstrated that the microhardness increased when increasing the density of cathode current, discharge voltage and the test object's temperature [6]. In experiment [7], the titanium nitriding under 480-500 °C did not change the microhardness of the near-surface layers.

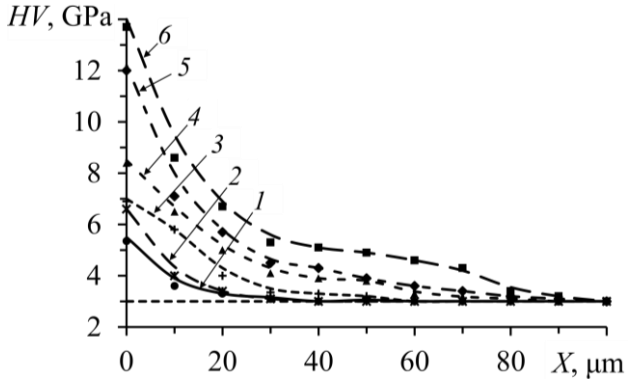

Figure 7. Microhardness profiles of the of the near-surface titanium layers BT1-0 under temperatures (°C) 550 (*1,2*), 650 (*3,4*) and 850 (*5,6*); *2,4,5* – backside of the test object; *1,3,6* – face side; dash line – object microhardness before nitriding [6].

The simulation results are presented in figure 8. The results of the research [14] at the temperature range of 540-610 °C were used to define the diffusion coefficient. Applying the extrapolation, the following values of the diffusion coefficient were obtained: $D(T = 550\ °C) = 5\times10^{-15}$ μm^2/s, $D(T = 650\ °C) = 4\times10^{-14}$ μm^2/s, $D(T = 850\ °C) = 7\times10^{-14}$ μm^2/s. The calculated distribution of the nitrogen relative concentration C/C_S after five hours of processing is presented in figure 8a, where C_S is the concentration of nitrogen atoms at the object face side. The concentration dependence on time for the face side and backside of the test object are presented in figure 8b.

As figure 7 shows, the values of the microhardness at the face and side of the test object differ slightly which points the core role of the nitrogen atoms in the titanium nitriding and the nitride layer formation. The depth of the hardened layer depends on the nitriding time and the object temperature. The lower values of microhardeness at the object face side (figure 7, curves 1 and 3) compared to the backside might be caused by the ion etching of the surface. This effect was not considered in the numerical simulation.

The comparing of the experimental results (figure 7) and the numerical diffusion simulation (figure 8) shows that the time-and temperature-dependent microhardness profile of the titanium surface and the nitrogen concentration are in agreement with each other. This means that the growth of the nitride layers is defined by the nitrogen atomic diffusion. The nitrogen atomic diffusion into titanium was well demonstrated by the diffusion model (3)-(4).

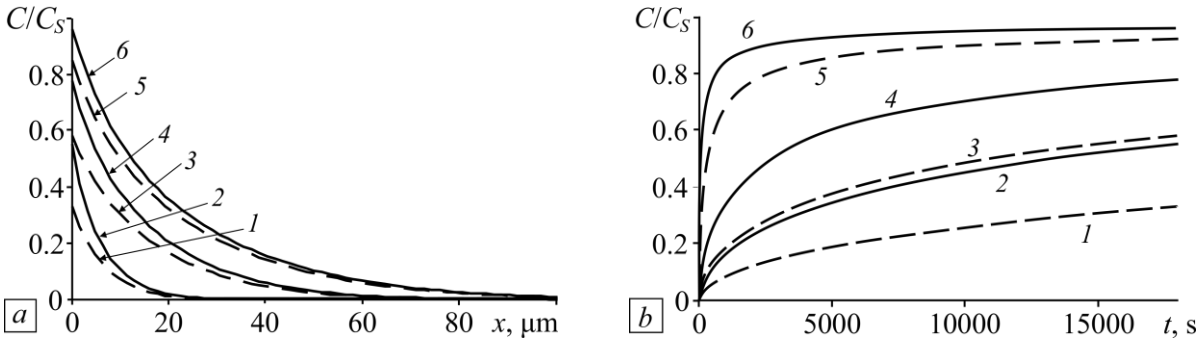

Figure 8. Calculated profiles of the nitrogen concentration in titanium (*a*) and its dependence on the processing time (*b*) under different temperatures (°C) 550 (*1,2*), 650 (*3,4*) and 850 (*5,6*) without considering the spraying surface by ions; *1,3,5* – test object backside; *2,4,6* – face side.

4. Conclusion

The numerical simulation of the plasma generation and the plasma-chemical nitriding covers the solution for the problems of the non-self-sustained discharge, gas ionization, thermal conductivity and diffusion. The model provides relations between main technological parameters such as gas pressure, electrical characteristics of a discharge, ion current density and the structure of the modified near-surface layer (the nitrogen concentration profile, the width of nitride layers and the diffusion zone) formed while nitriding metals or alloys by the non-self-sustained low-pressure glow discharge.

References

[1] Panajoti A 2003 *Fiz. Khim. Obr. Mater.* **4** 70–8
[2] Schanin P M, Koval N N, Goncharenko I M and Grigoriev S V 2001 *Fiz. Khim. Obr. Mater.* **3** 16–9
[3] Hosseini S R and Ashrafizadeh F 2009 *Vacuum* **83** (9) 1174–8
[4] Zagonel L F, Figueroa C A, Droppa J R and Alvarez F 2006 *Surf. Coat. Tech.* **201** (1-2) 452–7
[5] Berlin E V, Koval N N and Seidman L A 2012 *Plasma thermochemical surface treatment of steel parts* (Moscow: Tekhnosfera) p 462 (in Russian)
[6] Akhmadeev, Yu H 2007 *Non-self-sustained glow discharge with a hollow cathode for the nitriding of titanium* (PhD thesis, Institute of High Current Electronics SB RAS, Tomsk, Russia) Retrieved from http://www.dissercat.com/content/nesamostoyatelnyi-tleyushchii-razryad-s-polym-katodom-dlya-azotirovaniya-titana (in Russian)
[7] Akhmadeev Yu H, Lopatin I V, Koval N N, Schanin P M, Kolobov Yu R, Vershinin D S and Smolyakova M Yu 2010 *Modification of Materials with Particle Beams and Plasma Flows: Proc. 10th International Conference* (Tomsk, Russia, 19–24 September 2010) 228–31
[8] Lopatin I V, Schanin P M, Akhmadeev Y H, Kovalsky S S and Koval N N 2012 *Plasma Phys. Rep.* **38** (7) 583–9
[9] Koval T V, Lopatin I V, Nguyen B H and Ogorodnikov A S 2015 *Radiation and Nuclear Techniques in Material Science – Adv. Mater. Res.* **1084** 196–9
[10] Korolev Yu D, Frants O B, Landl N V, Shemyakin I A and Geyman V G 2013 *IEEE Trans. Plasma Sci.* **41** (8) 2087–96
[11] Pastuh I M 2006 *Theory and Practice of Nitriding in a Glow Discharge Without Hydrogen,* (Kharkiv: KIPT) p 364 (in Russian)
[12] Mufu Yan Qingchang Meng and Jihong Yan 2003 *J. Mater. Sci. Technol.* **19** (1) 164–6
[13] Bernal J, Medina A, Bejar L, Rangel S and Juanico A 2011 *International Journal of Mathematical Models and Methods in Applied Sciences* **5** (2) 395–403
[14] Sadliy T P, Milowa L G, Baranowa T A and Kurjatnikov S V 2004 *Physics of aerodisperse systems* **41** 124–9 (in Russian)